Relaxation Processes in Surface Excess Layers of Aqueous Solutions of Poly(ethylene oxide)

R. W. Richards* and M. R. Taylor

Interdisciplinary Research Centre in Polymer Science and Technology, University of Durham, Durham, DH1 3LE, U.K.

Received November 15, 1996; Revised Manuscript Received March 24, 1997[⊗]

ABSTRACT: The dynamic surface behavior of the surface excess film adsorbed at the air−liquid interface of dilute solutions of poly(ethylene oxide) has been investigated using surface quasielastic light scattering over a q range of 200 to 1300 cm^{-1}. Molecular weights of 15 000, 106 000 and 828 000 in 0.1%w/w solution in water were investigated. Capillary wave frequencies were close to simple predictions based on the density and surface tension of the solutions, whereas the dampings were higher than predicted, due to the extra surface viscosities of the adsorbed polymer. Light scattering data were further analyzed to yield the four surface viscoelastic parameters which are currently used to model the surface behavior—surface tension, γ_o, transverse shear viscosity, γ', dilational modulus, ϵ_o, and dilational viscosity, ϵ'—as a function of the capillary wave frequency. Variations in the dilational modulus and viscosity indicated the presence of a relaxation process in the surface film: this was fitted to a model describing the surface relaxation in terms of diffusion between the bulk solution and a subsurface layer. Including an adsorption barrier in the model enabled the quantitative description of the observed variation in both the dilational modulus and the dilational viscosity, and also provided a rationale for the negative dilational viscosities observed.

Introduction

Although techniques such as neutron reflectometry have considerably increased our understanding of the structure of polymer films at interfaces,[1] the dynamics of these systems are still poorly understood. Capillary waves—thermally induced surface motions which continually roughen a liquid surface—provide a means of examining the dynamic behavior of surface films. This occurs because a surface film behaves viscoelastically in response to the surface stresses caused by capillary waves. A number of different surface stress modes are possible,[2] but only two are relevant here: shear transverse to the surface and compression/dilation in the plane of the surface. The surface parameters of interest are the surface tension (γ_o) and the Gibbs elasticity or dilational modulus (ϵ_o). These two parameters have associated viscosities—the transverse shear viscosity (γ') and the dilational viscosity (ϵ'). An experimental technique which is able to measure the frequency spectrum of the capillary waves will be sensitive to these viscoelastic moduli and in principle afford a means for their evaluation.

In recent years surface quasi-elastic light scattering (SQELS) has been developed to study capillary waves.[3] As the technique has advanced it has been applied to a wide variety of systems: pure liquids, surfactant solutions, membranes and, more recently, polymers.[3] Major instrumental improvements have included the reliable provision of a local oscillator (for heterodyning),[4] correct allowance for the line width and other instrumental factors,[5] multiphoton counting,[6] and full unbiased fitting to the complete spectrum of scattered light.[7]

Poly(ethylene oxide) (PEO) is a technically important and academically intriguing polymer. In aqueous solution it spontaneously forms an adsorbed film at the air−solution interface, i.e. a surface excess, because of its much lower surface tension relative to that of water. The equilibrium surface behavior of the polymer is well-known: a surface excess with a molecular weight independent surface pressure ($\gamma_{o,\text{pure water}} - \gamma_{o,\text{solution}}$) ca. 10 mN m^{-1} is formed for solution concentrations of between 0.1 and 10^{-3} %w/w.[8] Below this concentration range, the surface pressure decreases; above it, a further increase in the pressure is observed which is dependent on the molecular weight of the polymer.[8]

SQELS has previously been applied to various polymer film systems,[9−17] including some studies on PEO-containing copolymers and PEO homopolymer films, although different workers have studied different aspects of the systems. Sauer and Yu[17] investigated spread and adsorbed films of PEO using a similar molecular weight range to that used here but at much lower bulk polymer concentrations (10^{-4} to 10^{-3}%w/w) and found no difference in the adsorbed and spread film behavior. This conclusion was based on the apparently identical variation of the frequency and damping data: no further analysis to yield surface viscoelastic data was undertaken. Cao, Kim, and Cummings[14] have studied a range of concentrations of PEO of molecular mass 1×10^6 g mol^{-1} and compared their results with a model which describes the crossover from capillary wave to elastic wave behavior due to the viscoelasticity of the bulk fluid as the concentration is increased. Again, frequency and damping data only were presented. Previously we have investigated PEO spread films at a range of surface concentrations[9] and observed negative dilational viscosities above surface concentrations of 0.5 mg m^{-2}. Neutron reflectometry studies[18] have shown that at this surface concentration the PEO chains begin to penetrate significantly into the subphase. In the present case the adsorbed film forms a surface excess of 0.6 mg m^{-2} from the subphase,[19] so we might expect to observe negative dilational viscosities here as well.

What is clearly lacking is a study of how the dynamic surface behavior of adsorbed PEO changes as the capillary wave frequency is varied, i.e. the dispersion behavior. We can also take advantage of recent developments in the analysis of SQELS data[7] to extract surface viscoelastic parameters as a function of capillary wave frequency. In this paper we present the first survey of the surface behavior of adsorbed PEO across the full frequency range currently available to SQELS

* Author to whom correspondence should be addressed.
[⊗] Abstract published in *Advance ACS Abstracts,* May 15, 1997.

S0024-9297(96)01684-1 CCC: $14.00

at various molecular weights. First we give a brief review of the relevant SQELS theory and the apparatus. A presentation of the measured frequencies and dampings of capillary waves as a function of q, the scattering vector, for the three polymers in 0.1% aqueous solution follows. The light scattering data is then further analyzed in terms of four surface viscoelastic properties. The dilational surface properties in particular are examined in terms of models which have been advanced to describe relaxation modes due to diffusion of molecules between surface and bulk.

Theory

Detailed theoretical descriptions of capillary waves and SQELS have been published elsewhere;[3,7,20,21] hence only a précis of the relevant theory is given here. A free liquid surface or a liquid−liquid interface, even when macroscopically smooth, is rough on a microscopic scale due to thermal motions of its constituent atoms or molecules. These motions are generally described by resolving them into their Fourier components−capillary waves−which propagate on the surface with a particular wavenumber, q, frequency, ω_o, and damping, Γ. Generally the waves are of small amplitude (on the order of ångstroms), although the amplitude is temperature and interfacial tension dependent and thus can increase dramatically near critical points. Generally for SQELS the accessible wavelength ($=2\pi/q$) is on the order of 100 μm, and the associated frequency is on the order of 10^5 Hz.

The theory for surface waves at the interfaces of pure liquids is well established: the frequency and damping of the capillary waves in such a system are related by a dispersion equation to their wavenumber by the surface tension of the interface and the viscosities and densities of the two fluids forming the interface. In the present work, we deal only with the free surface of a liquid−the air−liquid interface. From the dispersion equation for the free surface of a pure liquid, there are two approximate but useful solutions in terms of the surface tension, γ, the liquid density, ρ, and the liquid viscosity, η:

$$\omega_o = \sqrt{\frac{\gamma}{\rho}q^3}\left(1 - \frac{1}{2Y^{3/4}}\right) \tag{1a}$$

and

$$\Gamma = 2\frac{\eta}{\rho}q^2\left(1 - \frac{1}{2Y^{1/4}}\right) \tag{1b}$$

with

$$Y = \frac{\gamma\rho}{4\eta^2 q} \tag{1c}$$

These are modified forms of equations originally due to Kelvin and Stokes.

Various descriptions for more complex systems, such as insoluble and soluble films at interfaces, surfaces of polymer gels, and solutions, have been proposed. Here we are concerned with an adsorbed polymer film at an air−water interface, and so the appropriate form for the dispersion equation is[22]

$$D(\omega) = [\eta(q - m)]^2 - \left\{\frac{\epsilon}{\omega}q^2 + i[\eta(q + m)]\right\}\left\{\frac{\gamma}{\omega}q^2 - \frac{\omega\rho}{q} + i[\eta(q + m)]\right\} \tag{2}$$

with $m = (q^2 + i\omega\rho/\eta)^{1/2}$.

In this case, in addition to the capillary waves, there are longitudinal (in-plane) oscillations, the dilational waves. In the same way that the capillary waves are mainly controlled by the surface tension, the dilational waves are influenced mostly by the dilational modulus ϵ. For low values of q (below roughly 1000 cm^{-1}) the dilational waves follow

$$\omega = \frac{\sqrt{3}}{2}\left(\frac{\epsilon^2 q^4}{\eta\rho}\right)^{1/3} \tag{3a}$$

and

$$\Gamma = \frac{1}{2}\left(\frac{\epsilon^2 q^4}{\eta\rho}\right)^{1/3} \tag{3b}$$

The dilational and capillary waves are coupled, and resonance effects are observed between the two waves. For low q (ca. 200 cm^{-1}) this resonance occurs at a ratio of dilational modulus to surface tension of 0.16, although a q dependence of this ratio is observed. Earnshaw has pointed out that the two sets of waves can in fact be described as coupled damped oscillators, and he has described theoretically and experimentally the situations for observing mode mixing.[23,24]

The presence of a film (be it surfactant or polymer) at the surface introduces dissipative effects extra to those due to the viscosities of the subphase. These dissipative effects can be incorporated into the surface tension and dilational modulus by expanding them as linear response functions[25]

$$\gamma = \gamma_o + i\omega\gamma' \tag{4a}$$

$$\epsilon = \epsilon_o + i\omega\epsilon' \tag{4b}$$

where γ_o and ϵ_o are the moduli for transverse shear and dilation of the surface, and the primed quantities are the associated viscosities. (N.b. from here on the transverse shear modulus will be referred to by the more widely accepted term surface tension.) The exact effect of the viscosities on the oscillations is complex, but approximately we can say that increasing the transverse shear viscosity increases the damping of the capillary waves and increasing the dilational viscosity increases the damping of the dilational waves. In this model of surface dynamics these four parameters determine completely the behavior of the waves on the surface.

The power spectrum of light scattered from the surface by the capillary waves is given by

$$P(\omega) = -\left(\frac{k_B T}{\pi\omega}\right)\mathrm{Im}\left[\frac{i\omega\eta(q + m) + \epsilon q^2}{D(\omega)}\right] \tag{5}$$

Since this expression for the spectrum contains the dispersion equation, it is possible to fit it to light scattering data in order to obtain all four surface viscoelastic parameters. Physically, although the light is scattered by the capillary waves only, because of the coupling between capillary and dilational waves it is possible to determine the dilational modulus and viscosity. The power spectrum is a skewed Lorentzian, with a maximum which is the frequency of the capillary wave

Table 1. Molecular Weights, Polydispersities and Relevant Solution Properties of the Ethylene Oxide Polymers Studied

$M_w/10^3$	M_w/M_n	viscosity at 20 °C/10^{-3} Pa s	static surface tension at 20 °C/mN m^{-1}
15	1.1	1.040	61.5
106	1.1	1.099	61.5
828	1.1	1.474	62.1

ω_o and a width proportional to the capillary wave damping Γ. Recording the scattered light in the time domain and using heterodyne correlation methods result in the correlation function having the appearance of a damped cosine function, with a frequency ω_o and a damping Γ.

Experimental Section

Materials. Three different molecular weights of PEO were used: the molecular weights and polydispersities are given in Table 1. The highest molecular weight PEO was supplied by Polymer Labs (Church Stretton, U.K.) and was used as supplied. The two lower molecular weight samples were prepared by anionic polymerization in THF, using diphenyl methyl potassium as initiator. Molecular weights and polydispersities of the dried polymers were determined by size exclusion chromatography using chloroform as the eluting solution, against PS standards.

Table 1 also includes pertinent solution characteristics. Solutions of concentration 0.1% w/w (1 kg m^{-3}) for each polymer were made in ultrahigh quality water (Elgastat UHQ, Elga, High Wycombe, U.K.). The density of each solution was measured using a digital density meter[26] to be the same as water to within 0.1%. Viscosities were measured with an Ubbelohde capillary viscometer to an accuracy of 0.5%. The static surface tension in each case was determined by the Wilhelmy plate method.

Surface Quasielastic Light Scattering. The SQELS apparatus has been described in detail elsewhere[9] so only brief details will be given here. Polarized light from a 100 mW diode-pumped YAG laser (cw, 532 nm) was focused on the water surface, the reflected and scattered light being collected by a mirror and directed toward a photomultiplier tube (PMT). An optical system of two lenses either side of a diffraction grating (10 μm lines separated by 150 μm) was placed in the beam before the water surface to provide a series of reference light sources for heterodyne correlation at the PMT. In a measurement one particular beam from the grating is selected, and this forms the reference beam for the light scattered from the main (undiffracted) beam at the same angle. By alignment on different beams, the scattering angle is varied and thus capillary waves of different q and frequency can be accessed. The reference beam intensity was adjusted with neutral density filters to be between 10^3 and 10^6 times greater than that of the scattered light. The pulses output by the PMT were sent to a Malvern 128 channel correlator (K7025) via a standard Malvern amplifier-discriminator package. The quality of the correlation function building up in the correlator could be assessed via a continuous output to an oscilloscope. After collection, data was downloaded to a PC for storage and analysis. For each q value investigated, at least 10 correlation functions were recorded, and each was analyzed individually. The results reported here are the average values, and the error bars are derived from the variation of the parameters from fitting the different correlation functions.

Results

Data Analysis. A typical recorded correlation function is shown in Figure 1: it has the appearance of a damped cosine, implying that the capillary waves decay in a damped oscillatory fashion. This correlation function is the Fourier transform of the power spectrum of the scattered light. Once recorded, two separate analyses were applied to the data. The first "phenomenological" fit fitted a function (eq 6) based on a damped

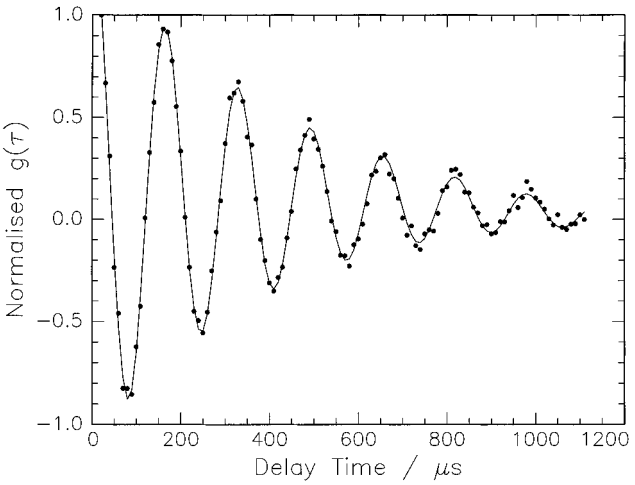

Figure 1. Typical measured correlation function (+) plus fit (—) for 0.1%w/w of 828 K PEO in water at q = 285 cm^{-1}.

$$g(\tau) = B - D\tau^2 + A\cos(\omega_o + \phi)\exp(-\Gamma t)\exp\left(\frac{-\beta^2\tau^2}{4}\right) \quad (6)$$

cosine to the correlation function recorded, to extract values of the frequency, ω_o, and damping, Γ, of the capillary waves.

In equation 6, β is an instrumental line width term[5] and the phase term, ϕ, accounts for deviations of the spectrum of scattered light from a Lorentzian. The amplitude of the correlation function is A, B is a background term, and $D\tau^2$ accounts for the effect on the correlation function of any external mechanical vibrations.

The second fitting method used in this work we term "spectral fitting", since it fits the correlation function with the Fourier transform of the theoretical power spectrum. This method, developed by Earnshaw and co-workers, has been described extensively elsewhere.[7] Initial estimates of the four surface viscoelastic parameters are supplied, and a theoretical power spectrum is calculated from these estimates, using eqs 2 and 5. This power spectrum is Fourier transformed to the correlation function and then compared with the data. This process is repeated iteratively until a specified tolerance level is reached and the program returns optimized values of the four surface viscoelastic parameters. It is important to realize that the meaning of the values returned by this method is restricted by the quality of the model dispersion equation used. Thus if the dispersion equation does not describe the system accurately, the returned values for the surface viscoelastic parameters may be "effective" values, incorporating more than one process. An effective parameter in the theoretical dispersion is one which reproduces all the observed phenomenon but where the phenomenon may be more accurately described by a better (but unavailable) theoretical expression.

The necessity of incorporating all four viscoelastic parameters in the spectral fitting procedure was investigated. It has been common to set γ' to zero; however, we have always found that unless we have a finite γ', the residuals in the fitting process are highly correlated. Furthermore, even if γ' is set to zero the values of ϵ' are still less than zero. We also remark here that solving the dispersion equation, eq 2, for Γ and ω_o

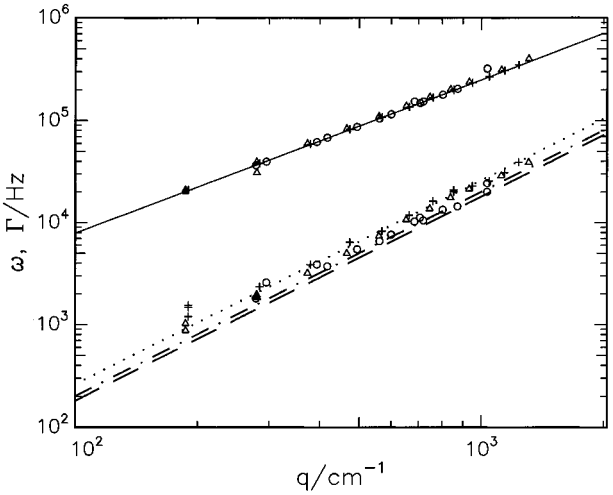

Figure 2. Fitted capillary wave frequencies and dampings for the 15 K (○), 106 K (△) and 828 K (+) PEO. Fitted error bars are smaller than the data points. The data are overlaid with the predictions for frequency from eq 1a (—) and for damping from eq 1b (---), (-·-) and (···) for, respectively, the 15 K, 106 K, and 828 K polymer solutions.

requires a finite positive γ' and a negative ϵ' to reproduce the observed capillary wave frequency and damping.

Frequency and Damping. Figure 2 shows the fitted values of ω_o and Γ for all three molecular weight polymers; note that slightly different q values were used for each polymer. This arises from small variations in the height of the liquid phase and thus the incident angle of the light beams on the surface. Also included are the lines calculated from the modified Kelvin and Stokes approximations for frequency and damping (eq 1) calculated for a liquid with the surface tension, density, and viscosity of the polymer solutions. For all of the data the error is smaller than the size of the symbol. Experimental frequencies are close to the predictions of equation 1a, and there is no discernible dependence on the molecular weight. The surface tensions and densities of the three polymer solutions are very similar, so this lack of molecular weight effect is expected. The closeness of the line to the frequency data also implies that the surface tension has the same value at high frequencies as the equilibrium value. This will be discussed further later.

The damping data are somewhat more complicated: there are clear deviations from the behavior predicted from eq 1b, and there is an evident molecular weight effect on the damping. To some extent this is expected because of the increase in the viscosity of the solution with polymer molecular weight, as can be seen by comparing the relative increase in viscosity and damping as polymer molecular weight increases. With reference to Table 1, the ratio of the viscosities of the three polymer solutions (low to high molecular weight) is 1:1.06:1.42. Taking one q value as an example (400 cm^{-1}) the ratio of the damping values are 1:1.01:1.31. This agreement is fair but does not account for all of the variation in damping. We note systematic deviations from the theoretical behavior which become more marked as the molecular weight of the dissolved polymer decreases. To establish the effect of the surface excess film on the capillary waves, we need to analyze the data in terms of the full dispersion equation.

Spectral Fitting. The data have also been analyzed for the four surface parameters—surface tension, γ_o,

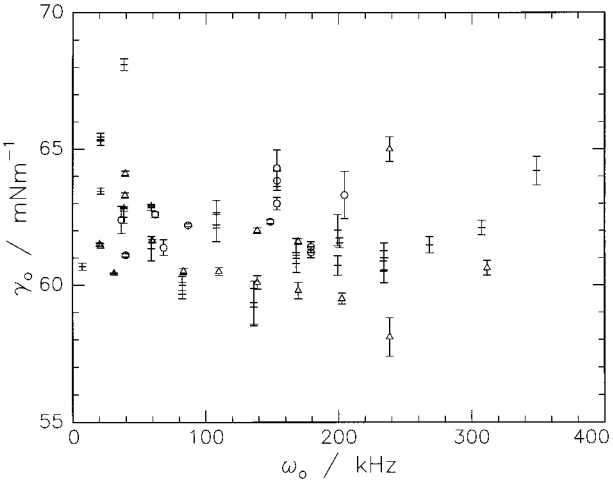

Figure 3. SQELS-determined values of surface tension for the 15 K (○), 106 K (△), and 828 K (+) polymer solutions.

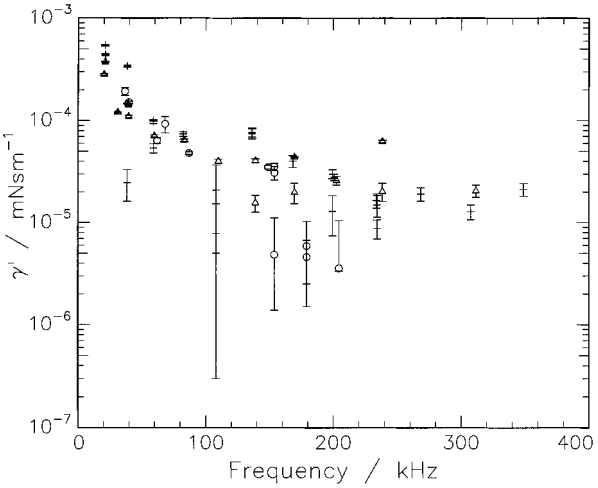

Figure 4. SQELS-determined values of transverse shear viscosity for the 15 K (○), 106 K (△), and 828 K (+) polymer solutions.

transverse shear viscosity, γ', dilational modulus, ϵ_o, and dilational viscosity, ϵ'. During the fitting procedure, it is possible to put bounds on the possible values the parameters can take. In the light of recent reports in the literature concerning negative surface viscosities,[27,28] we have allowed these parameters to explore negative and positive values during the fitting.

The fitted surface tension values for all three polymers for data taken over a range of q from 100 to 1100 cm^{-1} are shown in Figure 3 as a function of the capillary wave frequency. Although there is some scatter in the data, there is no evidence of any increase in surface tension with increased frequency, as might be expected if relaxation processes were occurring in the surface excess layer. Averaging all of the values together for each polymer solution gave surface tensions of 62.4, 61.2, and 62.1 mN m^{-1} respectively for the 15 K, 106 K, and 828 K polymers, with an estimated error of ±2 mN m^{-1}. There is thus no significant deviation from the static values of surface tension given in Table 1.

The value of the transverse shear viscosity for all three polymer solutions falls by 2 orders of magnitude with increasing capillary wave frequency from 20 to 400 kHz (Figure 4). This behavior is independent of the molecular weight of PEO. This reduction in viscosity with increasing frequency is reminiscent of relaxation behavior which has been observed in systems such as adsorbed monolayers of glycerol monooleate (GMO).[29]

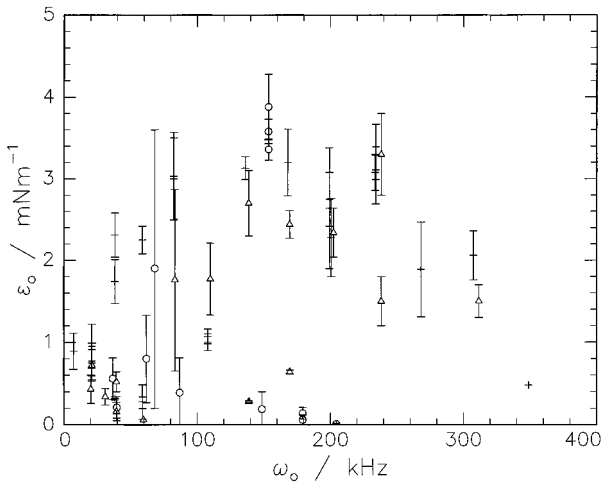

Figure 5. SQELS-determined values of dilational modulus for the 15 K (○), 106 K(△), and 828 K (+) polymer solutions.

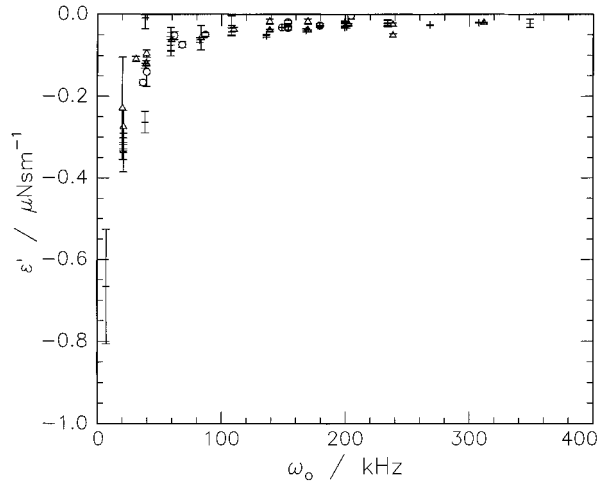

Figure 6. SQELS-determined values of dilational viscosity for the 15 K (○), 106 K (△), and 828 K (+) polymer solutions.

For all three polymer solutions, values of the dilational modulus show an increase from low values or zero at zero frequency to approximately 3 mN m^{-1} at a capillary wave frequency of 20 kHz (Figure 5). At still higher frequencies the modulus starts to decrease. This frequency dependence of the dilational modulus suggests the existence of at least one relaxation process: this should be accompanied by a reduction in the associated dilational viscosity as the frequency increases. In Figure 6 we do see a reduction in the magnitudes of the dilational viscosities of the three polymer solutions with increasing frequency; however, the sign of all of the measured viscosities is negative. This apparently unphysical result has been observed independently in other PEO-containing systems and low molecular weight surfactant solutions.[9,11,27,28]

Discussion

The simplest models describing viscoelastic relaxation in three-dimensional bulk solids are the Voigt−Kelvin and Maxwell models.[30] Both of these models attempt to describe viscoelastic behavior through some combination of elastic and viscous elements—springs and dashpots. These models have been applied to surface films by identifying γ_o (or ϵ_o) with the storage modulus $G'(\omega)$ and γ' (or ϵ') with $G''(\omega)/\omega$ where G'' is the loss modulus. The Voigt model predicts a frequency-independent γ_o (ϵ_o) and γ' (ϵ'), whereas the Maxwell model predicts a relaxation region where γ_o (ϵ_o) increases and γ' (ϵ') decreases. Although these models have been successfully applied to surface films,[9,10,27,29] they are only phenomenological: the notional "spring" and "dashpot" cannot easily be related to real physical parameters.

General *ab initio* theories for the viscoelasticity of surface films do not exist; however, for the particular case of the dilational properties of surfactant surface excess layers, various models have been developed describing relaxation effects due to processes such as surface−bulk exchange and micelle formation. These relaxation models have been reviewed elsewhere,[31] so we will concentrate only on the model which is relevant here: relaxation through diffusion-controlled exchange between the surface and bulk, considered with and without an adsorption barrier.

Lucassen-Reynders and Lucassen considered the effect of diffusion-controlled adsorption/desorption processes on the dilational properties of a surface excess film.[21] For measurements on insoluble films the static surface film elasticity or dilational modulus is related to the surface tension by

$$\epsilon_o = -\frac{\partial \gamma_o}{\partial(\ln \Gamma_S)} \tag{7}$$

where Γ_S is the surface concentration of the film. With a surface excess layer, however, the rate of compression or expansion of the layer is important and will affect the value of the dilational modulus measured, so this equation has to be significantly modified.

With the surface at some notional equilibrium, the surface concentration of material is given by the Gibbs equation

$$\Gamma_S = -\left(\frac{\partial \gamma}{\partial \mu}\right)_T \tag{8}$$

with μ being the chemical potential of the surface excess film. In fact, the surface is in constant agitation at a molecular level due to the capillary waves, which cause local surface concentration fluctuations. Material will adsorb and desorb as necessary to try to return the surface concentration everywhere to the equilibrium value given by eq 8. It is worthwhile pointing out that the transverse properties—surface tension and transverse shear viscosity—are not directly affected by this process. The reason for this can be easily seen if we consider a capillary wave to be made up of a pure transverse shear wave and a pure longitudinal compression wave. Shear of the surface in the direction normal to the plane of the surface (transverse shear) does not affect the surface concentration of polymer. In comparison, longitudinal compression causes variations in the surface concentration, above and below the equilibrium surface concentration given by the Gibbs equation. It is this surface concentration variation that diffusion acts to even out.

Lucassen-Reynders and Lucassen proposed that this adsorption/desorption process was controlled by diffusion between the bulk of the material and a layer immediately below the solution surface (this layer is not the surface excess layer). They considered that there was instantaneous equilibrium between the solution in this immediate subsurface layer and the local surface excess; i.e., adsorption or desorption occurred instantaneously from the immediate subsurface to the surface excess layer. The transport of polymer from the bulk of solution to the subsurface layer is diffusion controlled,

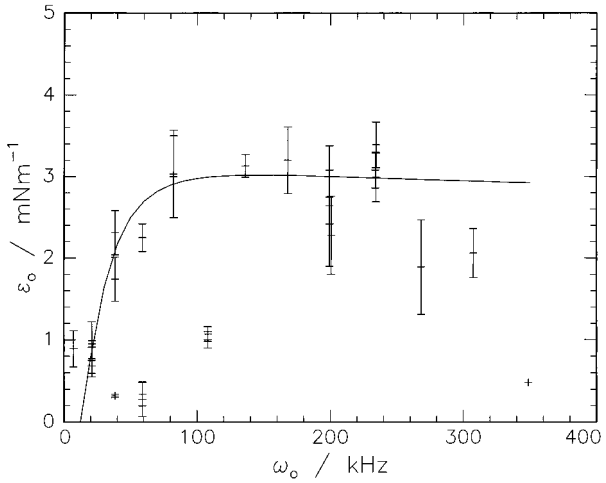

Figure 7. Fit of diffusional relaxation model to dilational modulus data for 828 K PEO.

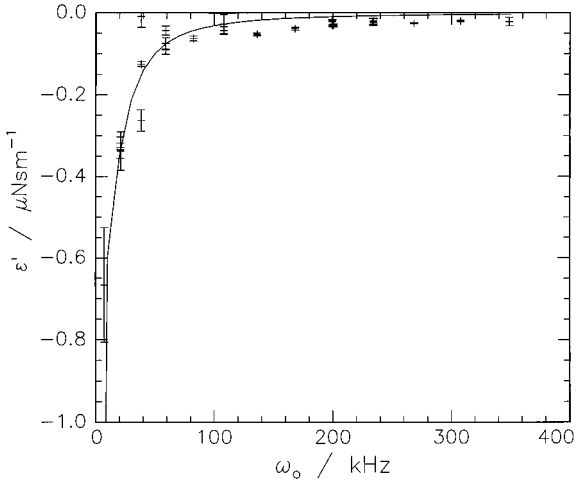

Figure 8. Fit of diffusional relaxation model to dilational viscosity data for 828 K PEO.

and there will be a characteristic time scale for this diffusion, determined by the diffusion coefficient. This leads to a frequency dependence of the dilational properties. If the characteristic time scale of the measurement of the dilational properties is longer than the time scale of the changes in concentration due to diffusion, the inhomogeneities in the polymer surface concentration caused by the capillary waves will be evened out and the dilational modulus measured will be unchanged from the static value. If, however, the characteristic time scale of the surface perturbation is much shorter than the diffusion time scale, the modulus measured is equal to a limiting modulus, ϵ_∞. Lucassen-Reynders and Lucassen developed expressions for the frequency dependence of ϵ_o and ϵ' in terms of ζ, a dimensionless diffusion parameter:

$$\epsilon_o = \epsilon_\infty \frac{1+\zeta}{1+2\zeta+2\zeta^2} \tag{9}$$

$$\epsilon' = \frac{\epsilon_\infty}{\omega_o} \frac{\zeta}{1+2\zeta+2\zeta^2} \tag{10}$$

$$\zeta = \frac{dc}{d\Gamma_S}\sqrt{\frac{D}{2\omega_o}} \tag{11}$$

$dc/d\Gamma_S$ is the inverse slope of the adsorption isotherm, and D is the diffusion coefficient of the polymer in bulk solution.

Equations 9 and 10 were fitted separately to dilational modulus and viscosity data as a function of frequency with ϵ_∞ and the term $((dc/d\Gamma_S)(D/2)^{1/2})$ as adjustable parameters of the fit. If the theory is applicable, we expect the values for these parameters from separate fits to the ϵ_o and ϵ' data to be the same, within error, for a particular PEO molecular weight. The fits of eqs 9 and 10 with the ϵ_o and ϵ' data for the 828 K PEO solution are shown in Figures 7 and 8. The fits to the data from the other two molecular weight polymers were of similar quality, and are not shown here. Fitting results are summarized in Table 2.

There is fair agreement between the fitted values derived from the dilational modulus and viscosity fits and a trend in the $((dc/d\Gamma_S)(D/2)^{1/2})$ term to lower absolute values at higher molecular weights. As Table 3 shows, this trend is due partly to the diffusion coefficient reducing by almost an order of magnitude as the molecular weight increases;[32−34] however, a small

Table 2. Fit Results from the Lucassen-Reynders and Lucassen Diffusion Model, Where Estimated Errors Are Given for Each Parameter Separately

	ϵ_∞/mN m^{-1}		$(dc/d\Gamma)(D/2)^{1/2}$	
	ϵ_o fit/±0.2	ϵ' fit/±2.0	ϵ_o fit/±27	ϵ' fit/±10
15 K	3.4	3.3	−186	−128
106 K	2.4	3.0	−179	−99
828 K	2.5	5.8	−112	−97

Table 3. Diffusion Coefficients[32−34] and Calculated Inverse Isotherm

		$dc/d\Gamma/10^7$ m^{-1}	
	$D/10^{-12}$ m^2 s^{-1}	ϵ_o fit	ϵ' fit
15 K	75	−3.0 ± 0.4	−2.1 ± 0.2
106 K	22	−5.4 ± 0.8	−3.0 ± 0.3
828 K	8	−5.6 ± 1.4	−4.8 ± 0.5

systematic decrease in $dc/d\Gamma_S$ with increasing molecular weight is still seen. This may be related to the molecular weight effect seen in the damping earlier (Figure 2), with systematic deviations from the theoretical behavior becoming more marked as the molecular weight of the polymer decreased.

One explanation for the negative viscosities observed lies within the Lucassen-Reynders and Lucassen theory. Examination of eq 9 and 10 shows that if $-1 < \zeta < 0$, then $\epsilon_o > 0$ with $\epsilon' < 0$, which is the situation observed here. As has been shown elsewhere,[28] in this situation the dilational modulus increases rapidly with increasing frequency to a maximum, and then declines slowly as the frequency increases further. This behavior, which is observed in our data, only occurs in the case of $-1 < \zeta < 0$. Given that a negative diffusion coefficient is unphysical, $dc/d\Gamma_S$ must be negative: this can occur if the surface concentration Γ_S and the immediate subsurface bulk concentration c are assumed to have a sinusoidal variation (due to the capillary waves) with some phase lag, ϕ, between the Γ_S and c variations. Writing

$$\frac{dc}{d\Gamma_S} = \frac{dc/dt}{d\Gamma_S/dt} \tag{12}$$

and

$$c = c_o e^{i\omega_o t} \qquad \Gamma = \Gamma_o e^{i\omega_o(t-\phi)} \tag{13a,b}$$

then

$$\frac{dc}{d\Gamma_S} = \frac{c_o}{\Gamma_o} e^{i\omega_o \phi} \tag{14}$$

Γ_o and c_o are the amplitudes of the respective oscillations. If $\pi/2 < \omega_o \phi < 3\pi/2$ then $dc/d\Gamma_S$ will be negative, as required.

This argument has been used previously[28] when explaining SQELS determined negative viscosities for aqueous solutions of long chain alcohols. However, it was pointed out that as the frequency increases the phase term ϕ will increase, causing the sign of $dc/d\Gamma_S$ to change. Here the frequency changes by over an order of magnitude; however, the dilational viscosity is always negative, implying that $dc/d\Gamma_S$ is always negative. Hence although the Lucassen-Reynders and Lucassen model can be used to fit the data, it is believed that this model is an incomplete description. One extension is to include specifically the effect of an adsorption barrier in the equations describing the dispersion of ϵ_o and ϵ'. In terms of the modulus of the complex dilational modulus ($|\epsilon| = [\epsilon_o^2 + (\omega\epsilon')^2]^{1/2}$) and the tangent of the complex plane phase angle ($\omega_o\epsilon'/\epsilon_o = \mathrm{Im}[\epsilon]/\mathrm{Re}[\epsilon]$), the relaxation equations are[31]

$$\frac{|\epsilon|}{\epsilon_\infty} = \frac{\sqrt{(1 + 2\beta\zeta + 2\beta^2\zeta^2 + \zeta)^2 + \zeta^2(1 + 2\beta\zeta)^2}}{(1 + \beta\zeta + \zeta)^2 + \zeta^2(1 - \beta)^2} \tag{15}$$

$$\frac{\mathrm{Im}[\epsilon]}{\mathrm{Re}[\epsilon]} = \frac{\zeta(1 + 2\beta\zeta)}{(1 + \zeta + 2\beta\zeta + 2\beta^2\zeta^2)} \tag{16}$$

The flux of molecules across the adsorption barrier is controlled by adsorption and desorption rates. In the model the effect of this barrier rate process enters into the relaxation equations via a dimensionless parameter β, which contains the desorption rate k_d:

$$\beta = \frac{\omega_o}{k_d} \tag{17}$$

In Figures 9 and 10 we have recast the data in Figures 5 and 6 in terms of the complex modulus $|\epsilon|$ (not normalized by ϵ_∞) and the tangent of the phase angle $\mathrm{Im}[\epsilon]/\mathrm{Re}[\epsilon]$. Note that due to the dilational viscosity being negative, the phase angle is also negative. Inspection of eq 16 shows that in order for the phase angle to be negative either ζ or β must be negative. The rate k_d must be positive, otherwise it is describing adsorption, so β must be always positive and hence ζ must be negative, as before with the diffusion-only model. With this extended model, there are now too many parameters for reliable fitting given the quality of the data, so qualitative comparisons only will be made. In Figures 11 and 12 we have plotted eqs 15 and 16 as a function of frequency for $\zeta = -200/\omega_o^{1/2}$ (the order of magnitude of the fitted values from Table 2) and k_d varying from 10^2 to 10^6. Below $k_d \approx 10^5$ the phase angle is positive across much of the frequency range studied, diverging for $\omega \approx k_d$. Above $k_d \approx 10^5$ the phase angle is negative with a positive modulus, and the curves compare well with the data. Included in Figures 11 and 12 are the curves for the diffusion only case: clearly these also describe the data well. Thus if an absorption barrier does exist, the rate associated with crossing the barrier must be high—ca 10^6 Hz—indicating that the energy height of the barrier must be relatively low.

The measurement of negative dilational viscosities is not unique to this system or this laboratory;[9,11,27,28]

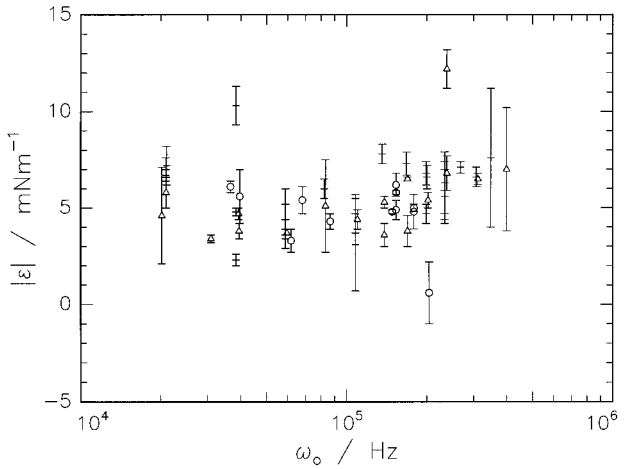

Figure 9. Complex modulus $|\epsilon|$ of the 15 K (○), 106 K (△), and 828 K (+) polymer solutions.

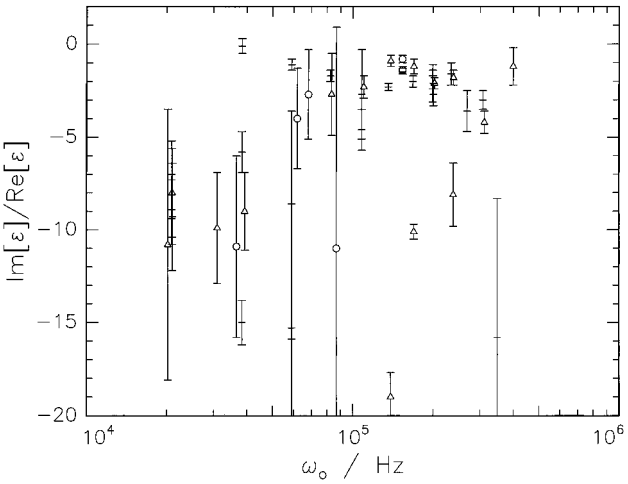

Figure 10. Phase angle $\mathrm{Im}[\epsilon]/\mathrm{Re}[\epsilon]$ for the 15 K (○), 106 K (△), and 828 K (+) polymer solutions.

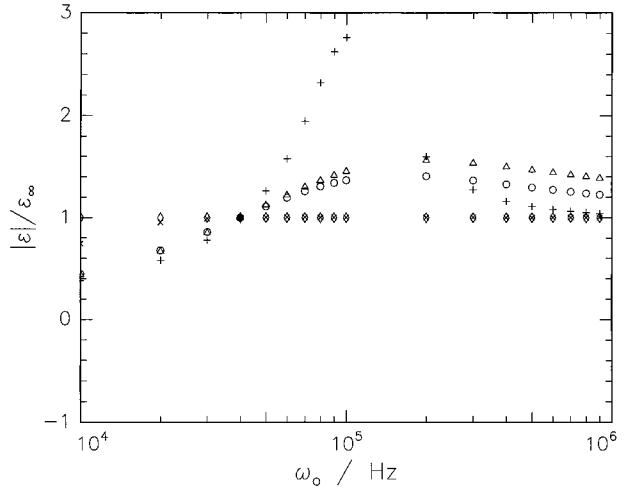

Figure 11. Theoretical predictions of $|\epsilon|/\epsilon_\infty$ from the diffusional relaxation model without adsorption barrier (○) and for the model with adsorption barrier, for $k_d = 10^2$ (◇), 10^4 (×), 10^5 (+), and 10^6 s^{-1} (△).

generally, they are observed in systems characterized by the surface active materials being soluble. The exception to this are recent experiments in this laboratory on some insoluble spread films (spread PEO, PMMA-*graft*-PEO[9,11]) which have also shown negative dilational viscosities, but only when the subphase becomes appreciably penetrated by one or more com-

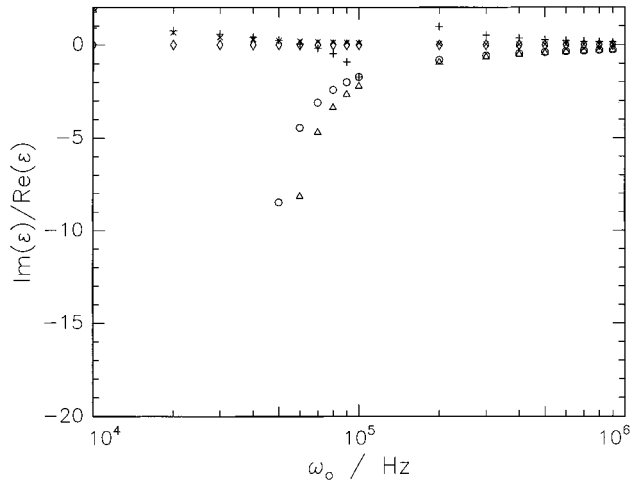

Figure 12. Theoretical predictions of Im[ϵ]/Re[ϵ] from the diffusional relaxation model without adsorption barrier (○) and with adsorption barrier, for $k_d = 10^2$ (◇), 10^4 (×), 10^5 (+), and 10^6 (△) s^{-1}.

ponents of the polymer. For the soluble surface excess layer considered here, it is reasonable to examine diffusion models for the surface relaxation and how they may explain negative dilational viscosities. Another way of rationalizing these data has recently been introduced,[24,35] where the dilational viscosity is thought to be an effective parameter because the dispersion equation does not properly describe the system; i.e. there are processes other than transverse shear and in-plane dilation contributing to the surface motion and thus affecting the capillary waves. This is quite possible in the insoluble spread film polymer systems where additional coupling can occur between the surface waves and chain motion.[11] Although a modified dispersion equation can be obtained which contains an additional coupling between the subphase and surface layer, as well as a bending modulus, these terms have an infinitesimally small contribution unless the surface tension is ultralow, i.e. circa 0.1 mN m^{-1}.

Conclusions

Using surface quasielastic light scattering we have examined three different molecular weight ethylene oxide polymers in dilute (0.1 wt %) solution in water. Capillary wave frequencies were in accord with simple predictions based on the density and surface tension of the bulk fluid. The dampings departed from the behavior expected for a simple fluid, indicating the presence of an adsorbed film: this departure was especially marked for the lower molecular weight polymers. The viscoelastic surface parameters, independently determined directly from the correlation function of the scattered light, showed relaxation behavior in both the transverse shear and dilation modes.

The frequency-dependent dilational modulus and viscosity data have been modeled using a relaxation model which ascribes the frequency dependence of the dilational modulus and viscosity to diffusion between the bulk solution and a subsurface layer. Inclusion of the concept of a barrier to adsorption between the subsurface and the surface allowed the model to describe the observed variation in both the dilational modulus and the dilational viscosity and also provided a rationale for the negative dilational viscosities observed. Small differences in the $dc/d\Gamma_S$ parameter were evaluated for the different polymer molecular weights, and these may be responsible for the deviations in damping from the Stokes predicted values.

Acknowledgment. We thank EPSRC for the financial support of the research project of which this work forms a part. Significant thanks are due to Tom Kiff for synthesis of the lower molecular weight PEO polymers. We are also grateful to Prof. J. C. Earnshaw of Queen's University, Belfast, U.K., for his continued interest in and encouragement of our work and his generous provision of fitting algorithms.

References and Notes

(1) Penfold, J.; Thomas, R. K. *J. Phys. Condens. Matter* **1989**, *2*, 1369.
(2) Goodrich, F. C. *J. Phys. Chem.* **1962**, *66*, 1858.
(3) Langevin, D. *Light Scattering by Liquid Surfaces and Complementary Techniques*; Dekker: New York, 1992.
(4) Hard, S.; Hamnerius, Y.; Nilsson, O. *J. Appl. Phys.* **1976**, *47*, 2433.
(5) Earnshaw, J. C.; McGivern, R. C. *J. Colloid Interface Sci.* **1988**, *123*, 36.
(6) Winch, P. J.; Earnshaw, J. C. *J. Phys. E: Sci. Instrum.* **1988**, *21*, 287.
(7) Earnshaw, J. C.; McGivern, R. C.; McLaughlin, A. C.; Winch, P. J. *Langmuir* **1990**, *6*, 649.
(8) Cao, B. H.; Kim, M. W. *Faraday Discuss.* **1994**, *98*, 245.
(9) Richards, R. W.; Taylor, M. R. *J. Chem. Soc., Faraday Trans.* **1996**, *92*, 601.
(10) Richards, R. W.; Rochford, B. R.; Taylor, M. R. *Macromolecules* **1996**, *29*, 1980.
(11) Richards, R. W.; Peace, S. K. *Polymer* **1996**, *37*, 4945.
(12) Tamada, K.; Miyano, K. *Jpn. J. Appl. Phys.* **1994**, *33*, 5012.
(13) Cao, B. H.; Kim, M. W.; Schaffer, H.; Cummings, H. Z. *J. Chem. Phys.* **1991**, *95*, 9317.
(14) Cao, B. H.; Kim, M. W.; Cummings, H. Z. *J. Chem. Phys.* **1995**, *102*, 9375.
(15) Kawaguchi, M.; Sano, M.; Chen, Y.-L.; Zografi, G.; Yu, H. *Macromolecules* **1986**, *19*, 2606.
(16) Kawaguchi, M.; Sauer, B. B.; Yu, H. *Macromolecules* **1989**, *22*, 1735.
(17) Sauer, B. B.; Yu, H. *Macromolecules* **1989**, *22*, 786.
(18) Henderson, J. A.; Richards, R. W.; Penfold, J.; Thomas, R. K.; Lu, J. R. *Macromolecules* **1990**, *26*, 4591.
(19) Lu, J. R.; Su, T. J.; Thomas, R. K.; Penfold, J.; Richards, R. W. *Polymer* **1996**, *37*, 109.
(20) Earnshaw, J. C.; Croxton, C. A. *Fluid Interfacial Phenomena*; John Wiley and Sons: New York, 1986.
(21) Lucassen-Reynders, E. H.; Lucassen, J. *Adv. Colloid. Interface Sci.* **1969**, *2*, 347.
(22) Langevin, D.; Meunier, J.; Chatenay, D. *Surfactants in Solution*; Plenum: New York, 1984; Vol. 3.
(23) Earnshaw, J. C.; McLaughlin, A. C. *Proc. R. Soc. London, A* **1991**, *433*, 663.
(24) Earnshaw, J. C.; McLaughlin, A. C. *Proc. R. Soc. London, A* **1993**, *440*, 519.
(25) Goodrich, F. C. *Proc. R. Soc. London, A* **1981**, *374*, 341.
(26) DMA 60/601 Density Meter, Anton Paar, Graz, Austria.
(27) Earnshaw, J. C.; Sharpe, D. J. *J. Chem. Soc., Faraday Trans.* **1996**, *92*, 611.
(28) Earnshaw, J. C.; McLaughlin, A. C. *Prog. Colloid Polym. Sci.* **1989**, *79*, 155.
(29) Earnshaw, J. C.; McGivern, R. C.; Winch, P. J. *J. Phys. Fr.* **1988**, *49*, 1271.
(30) Ferry, J. D. *Viscoelastic Properties of Polymers*, 3rd ed.; John Wiley and Sons: New York, 1980.
(31) van den Tempel, M.; Lucassen-Reynders, E. H. *Adv. Colloid Interface Sci.* **1983**, *18*, 281.
(32) Brown, W.; Stilbs, P.; Johnsen, R. M. *J. Polym. Sci., Polym. Phys. Ed.* **1983**, *21*, 1029.
(33) Kambe, Y.; Honda, C. *Polym. Commun.* **1984**, *25*, 154.
(34) Kambe, Y.; Honda, C. *Polym. Commun.* **1983**, *24*, 208.
(35) Hennenberg, M.; Chu, X.-L.; Sanfeld, A.; Velarde, M. G. *J. Colloid Interface Sci.* **1992**, *150*, 7.

MA961684R